Association of Two 3D QSAR Analyses. Application to the Study of Partial Agonist Serotonin-3 Ligands

Ronan Bureau, Cyril Daveu, Isabelle Baglin, Jana Sopkova-De Oliveira Santos, Jean-Charles Lancelot, and Sylvain Rault*

Centre d'Etudes et de Recherche sur le Médicament de Normandie, Université de Caen, 1, rue Vaubénard, 14032 Caen, France

Received June 5, 2000

CATALYST and COMFA, two software packages for 3D QSAR studies, were associated to correlate the three-dimensional structures of 75 serotonin 5-HT_3 ligands to their biological affinities. The conformational analysis and the influence of chemical function-based alignments (the basis of this association) on final results are discussed in this publication. These two analyses allow for precisely quantitating the weights of significant chemical groups or functions on the biological affinities.

INTRODUCTION

Serotonin (5-HT) is involved in multiple physiological functions or pathophysiological troubles at both the central and the peripheral level. Its receptor subtypes and their established or supposed physiological implications as well as their specific or nonspecific agonist or antagonist ligands are the subject of several recent reviews.[1−4] Among these subtypes, special attention was paid to the serotonin 5-HT_3 receptors largely because of the identification of highly selective and potent 5-HT_3 antagonists such as granisetron,[5] ondansetron,[6] and tropisetron[7] which are of high therapeutic interest in the prevention and treatment of emesis associated with anticancer chemotherapy.[8] 5-HT_3 antagonists or agonists could also be useful in the treatment of pain, memory impairment, depression, anxiety, drug addiction, and psychosis.

In our laboratory, the partial agonist affinity toward 5-HT_3 receptors of several series[9−11] including tricyclic piperazinopyrrolothienopyrazines (PPTP), piperazinopyridopyrroloppyrazines (PPPP), piperazinopyrroloquinolaxines (PPQ), piperazinopyridopyrroloquinoxalines (PPPQ), aminoalkyloximinopyrroloindoles (AAOPI), aminoalkyloximinothienopyrrolizines (AAOTP), and aminoalkyloximinopyrrolizines (AAOP) was demonstrated. The lack of information on specific 5-HT_3 agonists[12−16] and on their therapeutic potential makes these new compounds worth studying.

We recently defined a pharmacophore for 5-HT_3 partial agonists[17,18] from a three-dimensional (3D) quantitative structure−activity relationship (QSAR) approach (CATALYST[19] program). This first geometric fit procedure is efficient when a 3D pattern recognition is considered, but it is limited as far as the analysis of more subtle chemical phenomena is concerned. To achieve this, another 3D-QSAR method such as CoMFA, powerful in rationalizing binding sets of drug molecules, can be very useful. In this publication, our original 3D pharmacophore was used to carry out a chemical function-based alignment and to select the conformers (the two crucial steps of a CoMFA analysis). In the absence of three-dimensional data on the biological receptor, the chemical function-based alignment seems to be the most interesting approach to generate input data for 3D-QSAR studies. Previously, we published a CoMFA study of pyrrolothienopyrazines, with one reference compound as template for the alignment, leading to a q^2 value of 0.46.[17] Others recently published a comparative molecular field analysis of arylpiperazines (serotonin-3 antagonist)[20] with *d*-tubocuranine as template for the alignment. The differences with this present study relate (1) to the technique of selection of conformers and (2) in the former the consideration of only one series of compounds and in the latter the consideration of antagonists. In addition to these CoMFA studies, several publications[20−22] report different values for the dihedral angle between the aromatic and the piperazine group. Herein, we analyze the differences between the models obtained by molecular mechanics (CATALYST), molecular dynamics with a semiempirical program (MNDO94 with PM3 as Hamiltonian), and X-ray crystallographic data.

MATERIALS AND METHODS

CoMFA Strategy/Methodology. The CoMFA[23] studies were carried out on 75 compounds (see Table 1) corresponding to nine chemical series. The biological affinities of these compounds cover 8 orders of magnitude. The approach was carried out in three steps including the following: (i) the generation of a conformational model for each compound, (ii) the definition of an alignment, and (iii) the partial least-squares (PLS) analysis to correlate steric and/or electrostatic fields with the biological affinities.

Conformational Model Analysis. The conformational analysis was carried out by a systematic search method. The geometry was built with the CATALYST 2D/3D editor sketcher and minimized with the CHARMm-like force field implemented in the program.[24] Conformers were selected in the 0−20 kcal/mol range from the global computed minimum. A major drawback of this method lies in the fact that the conformational analysis of compounds having a piperazine group[18] generates chair conformations with substituents on the basic nitrogen always in the axial position. To go

* Corresponding author phone: (33) 2-31-93-41-69; fax: (33) 2-31-93-11-88; e-mail: rault@pharmacie.unicaen.fr.

10.1021/ci000058x CCC: $20.00
Published on Web 04/26/2001

Table 1. Structure and Biological Affinity ($-\log IC_{50}$) for Partial Agonists of 5-HT_3 Receptors

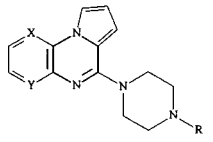

1-6

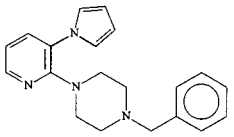

7

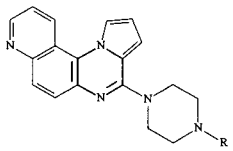

8-9

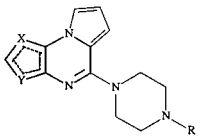

10-18

compound	X	Y	R^a	Affinity ($-\log IC_{50}$)
1	N	C	H	8.83
2	N	C	Allyl	11.40
3	N	C	Bn	12.09
4	N	C	4F-Bn	8.58
5	C	C	Bn	9.45
6	C	C	4F-Bn	8.62
7				7.34
8			Allyl	7.71
9			Bn	7.51
10	S	C	H	7.92
11	S	C	CH_3	6.09
12	S	C	Allyl	8.58
13	S	C	Bn	8.85
14	S	C	4F-Bn	7.67
15	C	S	CH_3	6.62
16	C	S	Allyl	9.04
17	C	S	Bn	8.34
18	C	S	4F-Bn	8.93

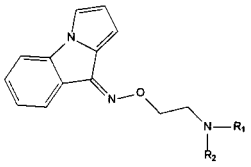

19-21

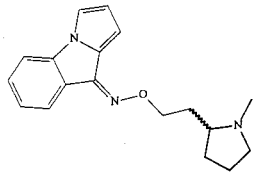

22

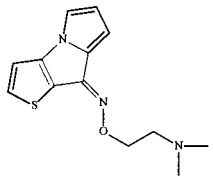

23

compound	R_1	$R_2{}^a$	Affinity ($-\log IC_{50}$)
19	H	H	6.66
20	CH_3	CH_3	8.24
21	H	Bn	6.54
22			7.85
23			8.46

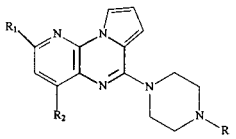

24-32

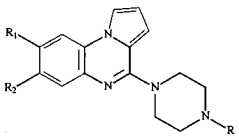

33-38

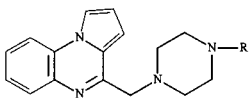

39

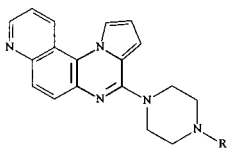

40

compound	$R_1{}^a$	$R_2{}^a$	R^a	Affinity ($-\log IC_{50}$)
24	H	H	CH_3	9.01
25	OCH_3	H	Bn	7.85
26	H	CH_3	Bn	5.52
27	OCH_3	H	4F-Bn	6.93
28	H	CH_3	4F-Bn	4.00
29	H	H	piperonyl	9.10
30	H	H	2,4-Cl-Bn	5.89
31	H	H	Ph	4.56
32	H	H	CO_2Et	4.55
33	H	Cl	Bn	9.54
34	Cl	H	Bn	7.69
35	H	Cl	4F-Bn	7.71
36	H	OCH_3	4F-Bn	8.18
37	H	CH_3	4F-Bn	7.87
38	H	Cl	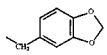	10.09
39			4F-Bn	5.59
40			piperonyl	7.55

Table 1 (Continued)

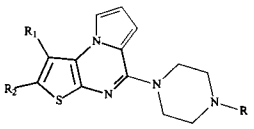

41-49

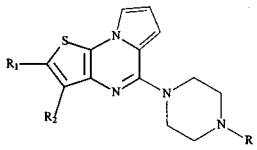

50-64

compound	R_1[a]	R_2[a]	R[a]	Affinity (-log IC_{50})
41	H	H	Ph-$_m$$CF_3$	4.13
42	H	H	2,4-Cl-Bn	5.38
43	H	H	3,4-Cl-Bn	5.93
44	H	H	piperonyl	8.99
45	H	Ph	CH_3	4.67
46	H	Ph	Ph-$_m$$CF_3$	2.76
47	Ph	H	Ph-$_m$$CF_3$	5.53
48	H	Ph	Bn	4.40
49	Ph	H	Bn	5.17
50	H	H	-$CH_2CH_2CH_3$	7.22
51	H	H	4-Cl-Ph	3.61
52	H	H	4-F-Ph	4.01
53	H	H	Ph-$_m$$CF_3$	5.80
54	H	H	2,4-Cl-Bn	7.78
55	H	H	3,4-Cl-Bn	5.64
56	H	H	-CH_2CH_2Ph-$_o$$CF_3$	3.57
57	H	H	-CH_2-CH=CH-Ph	6.70
58	H	H	-CH_2-Cyclopropyl	7.22
59	H	H	-$CO_2CH_2CH_3$	3.69
60	H	H	-$CH_2CO_2CH_2CH_3$	5.39
61	Ph	H	H	5.61
62	Ph	H	CH_3	4.72
63	Ph	H	Bn	3.23
64	CH_3	CH_3	Bn	5.44

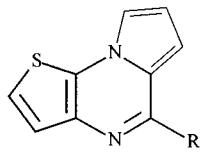

65-67

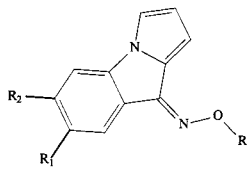

68-74

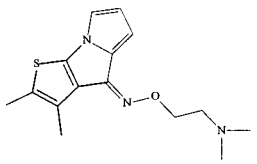

75

compound	R_1[a]	R_2[a]	R[a]	Affinity (-log IC_{50})
65				4.68
66				4.14
67			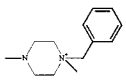	6.90
68	Cl	H	-$CH_2CH_2N(CH_3)_2$	7.07
69	Cl	H	-$CH_2CH(CH_3)N(CH_3)_2$	6.68
70	CH_3	H	-$CH_2CH(CH_3)N(CH_3)_2$	7.36
71	H	H	-$CH_2CH(CH_3)N(CH_3)_2$	8.28
72	H	Cl	-$CH_2CH(CH_3)N(CH_3)_2$	6.92
73	Cl	H		6.89
74	CH_3	H		7.43
75				6.68

[a] Bn = Benzyl, 4F-Bn : 4-fluorobenzyl, 2,4-Cl-Bn : 2,4-dichlorobenzyl, 3,4-Cl-Bn : 3,4-dichlorobenzyl

beyond this problem, a second step was carried out by adding equivalent equatorial conformations in the set of conformers, after minimization by molecular mechanics (CVFF force field).[25]

A comparison of the 3D structures obtained for compound **13**, the reference of our first 3D-QSAR study,[17] with MNDO94(PM3),[17] CATALYST (Figure 1, conformation which best fit the pharmacophore), and X-ray analysis (Figure 2) led to the following observations:

1. The 3D structures, resulting from the analyses carried out with the software MNDO94 and X-ray crystallographic data, present an excellent agreement for the dihedral angle

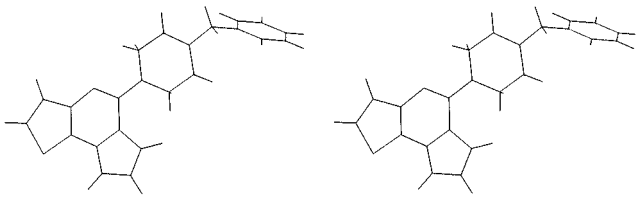

Figure 1. Conformation of compound **13** considered by CATALYST as the conformation which best fits the pharmacophore (stereopairs).

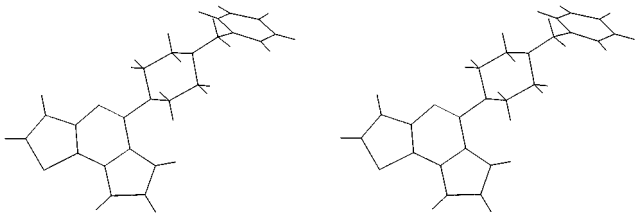

Figure 2. Representation of the conformation of compound **13** in the crystal structure (stereopairs).

between the piperazine and the tricyclic ring (8.8° vs 8.4°). This value determines (1) the height of the basic center toward the plane defined by the aromatic ring and (2) the orientation of the basic center (see previous pharmacophores[17,18,26]).

2. With CATALYST, the force field (CHARMm-like) defines the first nitrogen of piperazine with a sp^2 hydridation. This hydridation leads to a different value (30° vs 8.4°) compared to the previous one for the dihedral angle between the piperazine and tricyclic ring (conformation considered in this study); however, the piperazine keeps a chair conformation (Figure 1). It is the same situation for all the compounds generated by CATALYST (PPTP, PPPP, PPQ, and PPPQ series).

3. New 5-HT_3 antagonists were described recently.[20−22] Their compounds are close to our PPTP and PPQ series. Their pyridine derivatives have a *N*-methylpiperazine moiety attached to the 2-position of pyridine nucleus. The analyses of their models[22] for these last compounds show that the dihedral angle between pyridine and piperazine is around 65° (30° for our models). In this case, the basic center is in the plane defined by the aromatic ring.[22] If this last value is correct (however in disagreement with several crystallographic data),[17] the differences of activities with our compounds could be discussed on the basis of this observation (partial agonist vs antagonist).

4. For the disposition of the benzyl group on the basic nitrogen of piperazine ring (definition of the position of the hydrophobic group for the pharmacophore), the results obtained with CATALYST are in agreement with crystallographic data (−175° vs −177°). The dihedral angle obtained with MNDO94(PM3) is different (−64°).

From these observations, we demonstrate that the conformational analysis with CATALYST led to several problems, in relation to the CHARMm force field. This result could affect the quality of our previous pharmacophore.[18] However, this pharmacophore underlined the importance of five chemical features corresponding to one hydrophobic group, two hydrogen bond acceptors (named HBA PP), one positive ionizable site (a basic center), and one aromatic ring (see Figure 3). By considering the corrected data in relation to

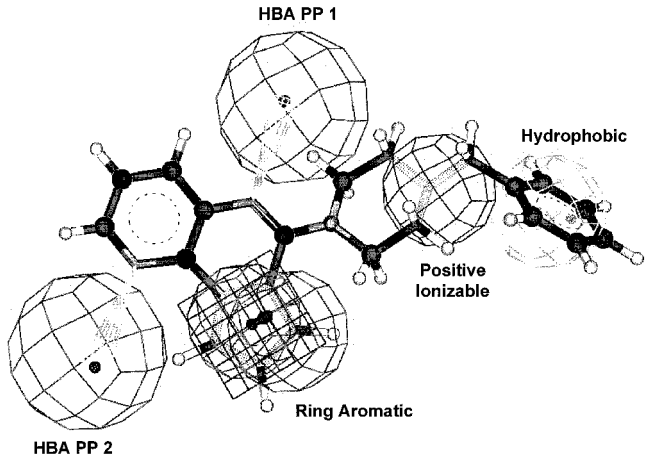

Figure 3. Respective positions for the different elements of the pharmacophore toward the structure of compound **3**.

the previous remarks and the conformation (CATALYST approach) of compound **13** which best fit the pharmacophore (Figure 1), the positions of the chemical features would not really change. Indeed, on these five chemical features, the height of the positive ionisable is not clearly modified (0.56 Å vs 0.67 Å), the orientation of the benzyl group and the position for the three others features are mostly conserved (see Figures 1 and 2). This last consideration led us to keep this pharmacophore for the following study.

Alignment Definition. The alignment rule was defined by a chemical function-mapping method and therefore based on a geometric fit of the chemical functions to the chemical features of the pharmacophore (Figure 1). The conformer selected for each compound corresponds to the conformation which best fits the pharmacophore. The average absolute derivatives of relative energy for all conformations (CVFF force field) are under 1 kcal/mol*Å. The final alignment was exported to CoMFA.[27] This selection method led to a problem for the series **68**−**74**. Indeed, the biological affinities were recorded for a mixture of the two configurations for every compound (we have yet no biological data for one configuration alone), and only one configuration Z or E was selected for each compound in this series. By preserving this unit, we have considered that substituents on the phenyl ring led to a decrease in the affinity for both Z- and E-isomer (compounds **20**, **23**, and **71**, with no substituent on the phenyl or thiophene ring, have the higher affinity in this family). Two compounds **65** and **66** have a particular alignment in relation to the fit of the amidine group on the positive ionizable site.

CoMFA Analysis. The partial charges for the compounds were calculated by two methods: Gasteiger-Huckel and Mulliken (MOPAC, AM1 as Hamiltonian). First, several probes were tested (SAMPLS)[28] with different charges and lattice spacing. In this analysis, two factors (steric and electrostatic) were analyzed with the appropriate probe atoms (van der Waals radius) and charges.

The best results were obtained with hydrogen as probe atom (charge +1) and Mulliken charges (see Table 2). The increase in the steric contributions led to worse statistics (see Br and I vs H). The variation of the charge did not improve the results (with the two fields). The variation of probe spacing showed that the optimum situation, in terms of a number of descriptors and cross-validation results, was 2 Å.

Table 2. Results of the PLS Analysis with Different Situations

probe atoms	charge	probe spacing (Å)	type of charges[a]	ONC[b]	q^2
Csp^3	+1	2	GH	9	0.54
H	+1	2	GH	8	0.58
H	+1	1	GH	7	0.60
H	+1	3	GH	7	0.36
Osp^3	−1	2	GH	7	0.52
Br	+1	2	GH	7	0.51
Csp^3	+1	2	M	6	0.45
H	+1	2	M	7	0.62
H	+1	1	M	6	0.61
H	+1.5	2	M	7	0.61
H	+4	2	M	6	0.58
Osp^3	−1	2	M	6	0.49
Br	+1	2	M	5	0.54
I	+1	2	M	6	0.52
H	+1	2	M	5	0.36[c]
H	+1.5	2	M	6	0.42[c]
H	+2	2	M	9	0.52[c]

[a] GH: Gasteiger-Hückel; M: Mulliken charge. [b] ONC: optimal number of components. [c] Electrostatic fields only.

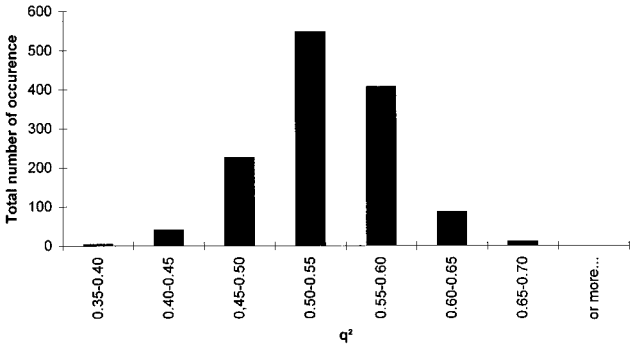

Figure 4. The q^2 values (Csp^3 as probe atom) observed for different orientations of the 75 compounds. The molecular aggregate was systematically rotated by 30° at a time around *x*, *y*, and *z* axes.

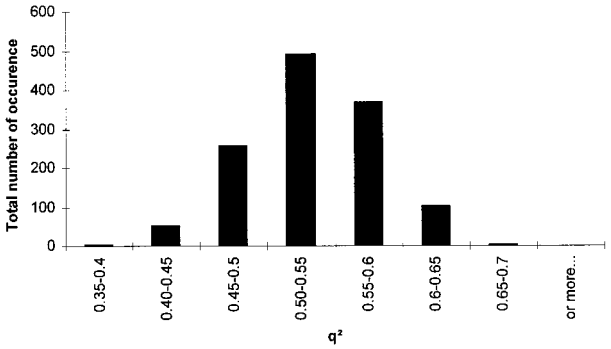

Figure 5. The q^2 values (H as probe atom) observed for different orientations of the 75 compounds. The molecular aggregate was systematically rotated by 30° at a time around *x*, *y*, and *z* axes.

With the electrostatic fields alone, an improvement of the predictive quality of the equation was observed when the charge increase.

Recently, some authors[29] found that the resulting q^2 values may vary greatly depending on the orientation of rigidly aligned molecules on the user terminal. We have investigated this phenomena for two probe atoms (Csp^3 and H). The variation of the q^2 values is represented in Figures 4 and 5.

These analyses show a close distribution of q^2 values whatever the probe atom (average q^2 values of 0.53). The best q^2 value was obtained with Csp^3 (0.66 vs 0.65 (H)).

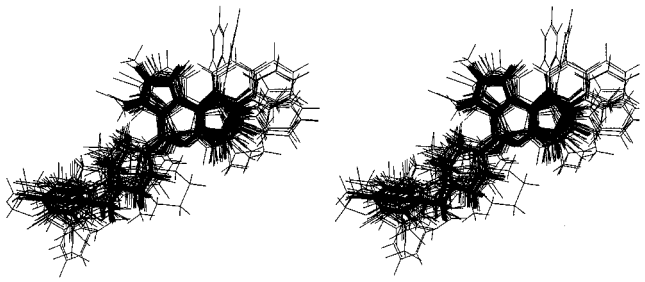

Figure 6. Orientation of the aligned compounds inside the lattice corresponding to the best q^2 value (orientation 1, stereopairs).

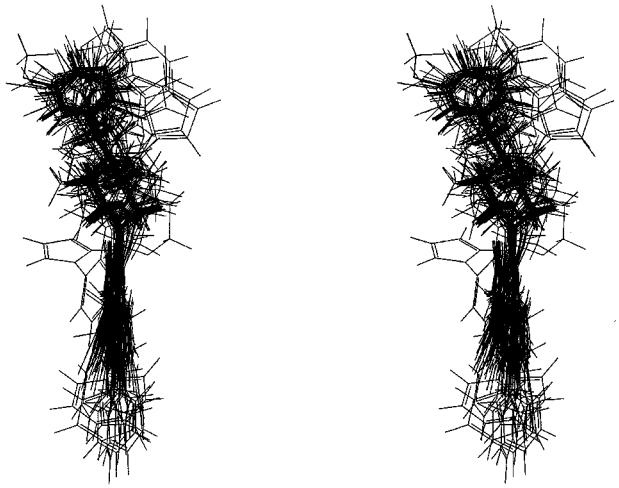

Figure 7. Orientation of the aligned compounds inside the lattice corresponding to the worst q^2 value (orientation 2, stereopairs).

Cross-validation analysis with these orientations led to the same trend (q^2 values of 0.62 (seven components) with H and 0.65 (five components, 0.67 with eight components) for Csp^3). In CoMFA, the steric and electrostatic fields, which theoretically form a continuum, are sampled on a fairly coarse grid.[29] As a result, these fields are represented inadequately, and the results are not strictly reproducible. Cramer et al. claimed that decreasing the grid spacing increases the adequacy of sampling.[30] We analyzed this assumption on the opposite results corresponding to orientation 1 ($q^2 = 0.66$, see Figure 6) and orientation 2 ($q^2 = 0.38$, see Figure 7). In agreement with Cramer's observation, a grid spacing of 1 Å improves the statistics for orientation 2 (0.48 vs 0.38), but those (0.62 vs 0.66) for orientation 1 decrease. The comparison of the electrostatic and steric fields for these two orientations led us to test the modification of the cutoff values. Indeed, a cutoff value of 300 kcal/mol for steric and electrostatic field led to a q^2 value of 0.59 for orientation 2 (six components, 2 Å for the grid spacing).

From this analysis, Csp^3 as the probe atom and orientation 1 were selected. The probe atoms were placed every 2 Å in all the three dimensions of the defined region. A cutoff of 30 kcal/mol was used for the steric and electrostatic interactions. During the PLS analysis, CoMFA_STD was used for scaling. A leave-one-out cross-validation was carried out to test the predictive quality of our equation. A minimum sigma of 2 kcal/mol was used during the cross-validation test and to calculate the final PLS equation.

Biological Affinities. Receptor binding assays were conducted using methods reported previously.[3] The assays used NG 108-15 cells and [^{3}H]BRL43694 and ICS 205930

Table 3. Experimental and Predicted Values with and without Cross-Validation

		cross-validation $-\log(IC_{50})$		final model $-\log(IC_{50})$	
compds	exptl $-\log(IC_{50})$	calcd	residuals	calcd	residuals
1	8.83	9.705	−0.875	9.087	−0.257
2	11.40	9.854	1.546	10.281	1.119
3	12.09	10.238	1.852	10.501	1.589
4	8.58	9.389	−0.809	9.141	−0.561
5	9.45	10.620	−1.170	9.964	−0.514
6	8.62	8.482	0.138	8.584	0.036
7	7.34	6.662	0.678	7.685	−0.345
8	7.71	8.336	−0.626	7.991	−0.281
9	7.51	6.744	0.766	7.420	0.090
10	7.92	7.113	0.807	7.133	0.787
11	6.09	7.442	−1.352	7.097	−1.007
12	8.58	8.758	−0.168	8.204	0.386
13	8.85	7.189	1.661	7.555	1.295
14	7.68	7.134	0.546	7.314	0.366
15	6.62	6.742	−0.122	6.962	−0.342
16	9.04	9.220	−0.180	8.633	0.407
17	8.34	8.458	−0.118	7.969	0.371
18	8.92	7.299	1.621	7.597	1.323
19	6.66	8.122	−1.462	6.974	−0.314
20	8.24	7.315	0.925	7.662	0.578
21	6.54	7.929	−1.389	7.372	−0.832
22	7.85	7.409	0.441	7.987	−0.137
23	8.46	7.289	1.171	8.430	0.030
24	9.01	9.161	−0.151	9.191	−0.181
25	7.85	7.377	0.473	7.932	−0.082
26	5.52	5.323	0.197	4.986	0.534
27	6.93	8.420	−1.490	7.593	−0.663
28	4.00	4.982	−0.982	4.351	−0.351
29	9.10	8.801	0.299	9.317	−0.217
30	5.89	5.608	0.282	5.730	0.160
31	4.56	6.863	−2.303	5.444	−0.884
32	4.55	5.686	−1.136	4.920	−0.370
33	9.54	8.775	0.765	9.227	0.313
34	7.69	8.805	−1.115	8.605	−0.915
35	7.71	8.991	−1.281	9.064	−1.354
36	8.18	7.324	0.856	7.905	0.275
37	7.87	7.957	−0.087	8.123	−0.253
38	10.09	9.465	0.625	10.296	−0.206
39	5.59	4.749	0.841	5.232	0.358
40	7.55	5.862	1.688	7.480	0.070
41	4.13	5.857	−1.727	4.831	−0.701
42	5.38	5.976	−0.596	5.182	0.198
43	5.92	6.432	−0.512	5.372	0.548
44	9.00	8.264	0.736	8.669	0.331
45	4.68	4.239	0.441	4.465	0.215
46	2.77	1.666	1.104	2.925	−0.155
47	5.53	4.255	1.275	5.211	0.319
48	4.40	4.931	−0.531	4.381	0.019
49	5.17	7.291	−2.121	5.205	−0.035
50	7.22	7.755	−0.535	7.524	−0.304
51	3.60	4.738	−1.138	3.752	−0.152
52	4.01	3.405	0.605	3.687	0.323
53	5.80	4.163	1.637	4.958	0.842
54	7.77	6.309	1.461	7.424	0.346
55	5.64	6.654	−1.014	5.526	0.114
56	3.57	6.106	−2.536	3.535	0.035
57	6.70	8.134	−1.434	7.410	−0.710
58	7.22	6.256	0.964	6.728	0.492
59	3.70	4.756	−1.056	4.167	−0.467
60	5.39	7.041	−1.651	5.977	−0.587
61	5.60	3.750	1.850	4.592	1.008
62	4.72	4.911	−0.191	4.502	0.218
63	3.23	5.051	−1.821	3.769	−0.539
64	5.44	6.611	−1.171	6.288	−0.848
65	4.68	4.679	0.001	4.412	0.268
66	4.14	5.208	−1.068	3.648	0.492
67	6.89	8.591	−1.701	7.772	−0.882
68	7.07	6.501	0.569	7.214	−0.144
69	6.68	7.503	−0.823	7.154	−0.474
70	7.36	6.710	0.650	7.017	0.343
71	8.28	7.151	1.129	7.721	0.559
72	6.92	7.208	−0.288	7.129	−0.209
73	6.89	6.575	0.315	7.263	−0.373
74	7.43	7.239	0.191	7.469	−0.039
75	6.68	7.128	−0.448	6.750	−0.070

for nonspecific binding. The concentrations of the radioligands used in competition studies were approximately equal to the Kd of the binding system. The affinity of the ligands was expressed as $\log(IC_{50}) \pm$ SEM (concentration inhibiting 50% of the specific binding) and calculated using LUNDON2 software.[31] The results obtained are reported in Table 1.

Table 4. Results of the CoMFA Analysis

cross-validation (steric and electrostatic)			final equation (five components)	
number of components	q^2	s	r^2	s
1	0.297	1.633	0.913	0.590
2	0.474	1.423		
3	0.574	1.29		
4	0.611	1.24		
5	0.645	1.193		
6	0.654	1.188		
7	0.665	1.176		
8	0.673	1.171		
9	0.670	1.186		

RESULTS AND DISCUSSION

The statistical results are summarized in Tables 3 and 4 and represented in Figures 8 and 9. The contribution was 43.5% for the steric fields and 56.5% for the electrostatic fields (final equation). The predictive quality is represented by the leave-one-out cross-validation results (q^2 values, see Table 4). Three compounds had a prediction error greater than 2 orders of magnitude (see Table 3, values in bold) which could be explained by their structures. For compounds **31** and **49**, the presence of four features of the pharmacophore (HBA1, HBA2, aromatic, and basic center for **31**; HBA2, aromatic, hydrophobic, and basic center for **49**) led to a predicted affinity close to 7 ($-\log IC_{50}$). The decrease of affinity due to a phenyl substitution on the basic center (**31**) and on the tricyclic ring (**49**) could not be considered during cross-validation because these substitutions are unique in the training set (**47** has also this substitution (**47** vs **49**), but in its structure only three characteristics of the pharmacophore are present). The same situation was observed for compound **56** which has three important features in its structure leading to a predicted affinity close to 6 ($-\log IC_{50}$).

Four CoMFA contour maps were analyzed to explain the statistical results. These maps show regions where differences in molecular fields are associated with differences in biological activity. These contour graphs concerned the probe atoms associated with the significant values of standard deviation *electrostatic or steric coefficients during the cross-validation analysis (orientation 1 and orientation 2 corresponding to the best and worst statistics for the same alignment and training set). The values mapped on these graphs correspond to the contribution values (the data are percentages of the overall sum of absolute values in the fields). In this case, we have not positive or negative regions but a representation of the points contributing most heavily to the correlation. The importance of two areas, one close to the γ position of the pyridine feature (tricyclic ring) and the second close to the hydrophobic feature of the pharmacophore, were pointed out by considering the electrostatic fields (clear difference with orientation 2, see Figures 10 and 11). The analysis of predicted values differences between the two orientations showed that the influence of ester groups or p-CF_3 phenyl groups on the basic center were correctly modeled by the

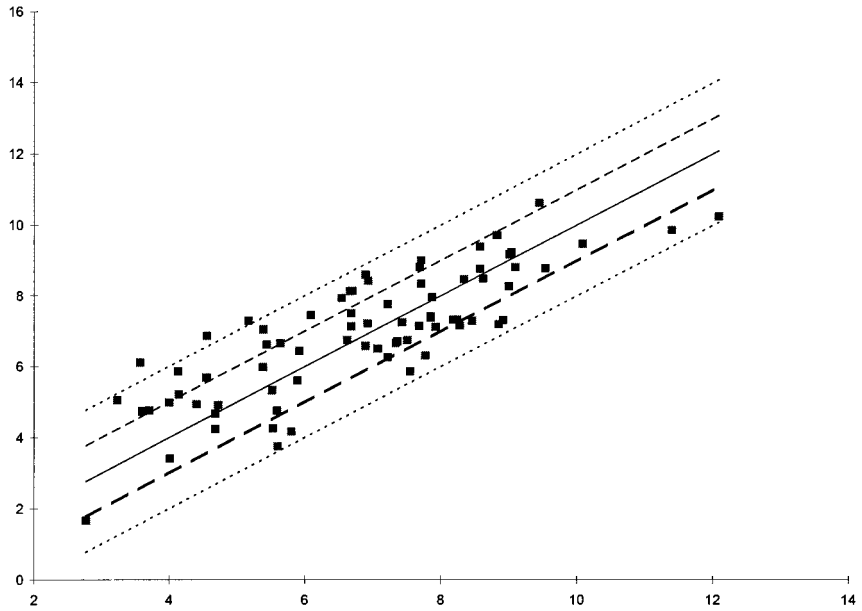

Figure 8. Measured activities versus predicted activities (cross-validation).

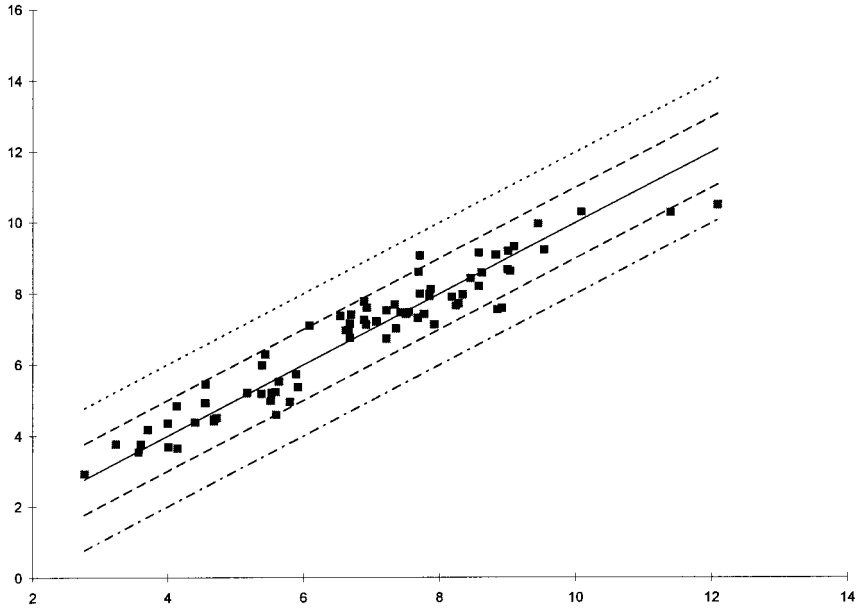

Figure 9. Measured activities versus predicted activities (without cross-validation).

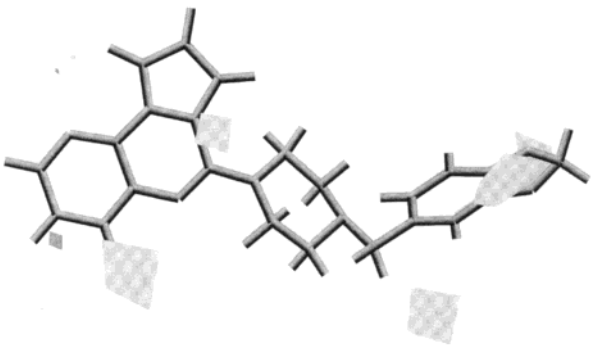

Figure 10. Standard deviation*PLS coefficients contour plots of CoMFA electrostatic fields during cross-validation. Significant contribution regions for the orientation 1.

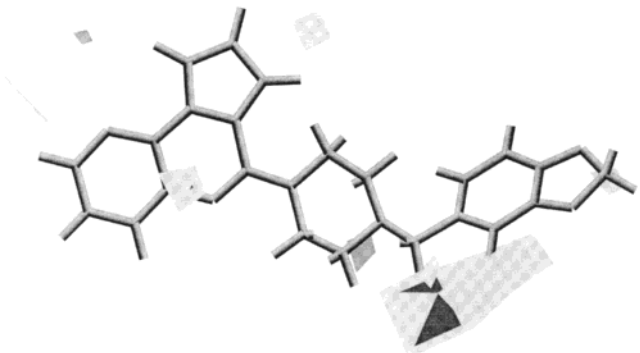

Figure 11. Standard deviation*PLS coefficients contour plots of CoMFA electrostatic fields during cross-validation. Significant contribution regions for the orientation 2.

definition of electrostatic contour maps in the region of the hydrophobic features (orientation 1). In the same way, the affinity differences for the series corresponding to compounds **41**−**64** led to the definition of contour close to the γ position of the pyridine. The definition of this region led to model more precisely the impact of the electrostatic variation in

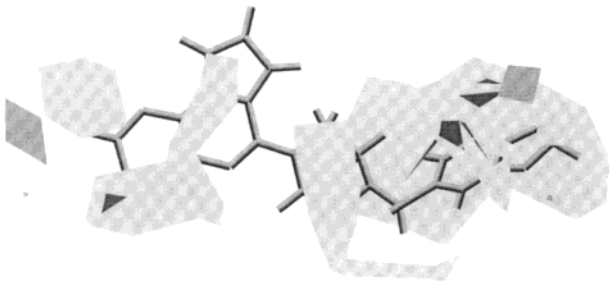

Figure 12. Standard deviation*PLS coefficients contour plots of CoMFA steric fields during cross-validation. Significant contribution regions for the orientation 1.

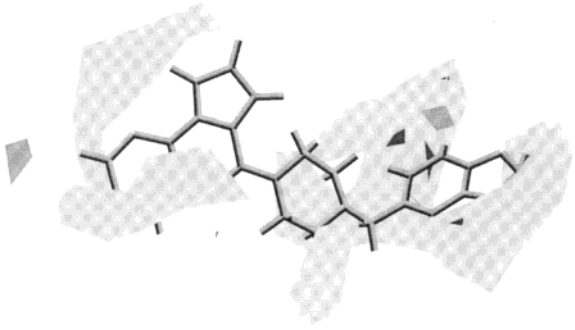

Figure 13. Standard deviation*PLS coefficients contour plots of CoMFA steric fields during cross-validation. Significant contribution regions for the orientation 2.

this region. For instance, the cross-validated affinities for compounds **41** and **53** are 5.85 and 4.16, respectively, for orientation 1 instead of 7.17 and 2.00 for orientation 2.

The steric contour maps (see Figures 12 and 13) show clearly the difficulty in analyzing the steric effect, particularly the hydrophobic region. Indeed this region is rich with CoMFA contours in relation to the structural diversity of our training set. CoMFA determines weights associated with a probe atom corresponding to a point in the lattice and not a sphere (representation of the features) as with CATALYST. Therefore, the predicted affinity is very sensitive to the variation of conformation for a compound. This led to a variation of 2 logarithmic units in relation to a slight variation of dihedral angles inside the series where R corresponds to allyl or benzyl (see the compound **13**). This problem is a direct result of the chemical function mapping method for the alignment, and it is the major difficulty in combining the CATALYST and CoMFA studies.

The significant variations of affinity with respect to specific chemical features are correctly modeled by this analysis. In particular, it correctly identifies the following: (1) the impact of chlorine atoms on the phenyl group (**30**, **42**, **43**, **54**, **55**; average predicted value of 6.17 ± 0.39); (2) the impact of an N-phenyl substitution of the piperidine (**41**, **51**, **52**, **53**; average predicted value of 4.54 ± 1.04); (3) the impact of a phenyl substituent on the tricyclic ring (**45**, **46**, **47**, **48, 61, 62**); (4) the steric impact of a methyl group on R_2 (**26**, **28**); and (5) the importance of the hydrophobic benzyl group on the piperazine. In contrast, this analysis does not explain the following: (1) the biological results for compounds **49** and **63** which are surprising by considering the data obtained for compounds **45**, **46**, **47**, **48**, **61**, and **62**; (2) the fact that a chlorine or a methyl group (position R_1 and R_2) on tricyclic piperazinopyrroloquinolaxines alters the biological activity (see the predicted affinity for **5** and **6** vs **33**, **34**, **35**, **37**); and (3) the influence (see **2**, **3**, **5**) of one hydrogen bond acceptor group (named HBA PP2 in the pharmacophore) in contrast to the previous study with CATALYST.

CONCLUSION

The first part of this study showed the difficulty in obtaining correct molecular models from the CATALYST software (CHARMm force field). However, comparison of conformations obtained with CATALYST, crystallographic data, and other studies led us to keep the partial agonist 5-HT_3 pharmacophore. From this pharmacophore, which forms the basis of the association of the two 3D QSAR studies, a structure−activity relationship starting from several families of compounds was established. In relation to this method, the variation of the chemical set orientation inside the regions led to difficulties for a CoMFA study like those observed in the hydrophobic region. Otherwise, the same trends observed with CATALYST were obtained for the definition of weights attributed to steric and/or electrostatic regions except for the HBA PP2 feature. Indeed, each feature of the CATALYST pharmacophore seems to correspond to a CoMFA region leading to an increase of affinity of approximately 2 logarithmic units. CoMFA modulate the predictive affinity by the definition of specific steric and/or electrostatic constraints around these regions. These results showed clearly the value to use CoMFA to quantitate the predictive affinity obtained from the fit between chemical groups and the features of the CATALYST pharmacophore.

ACKNOWLEDGMENT

The authors thank the "Réseau Interrégional Normand de Chimie Organique Fine" for the financial support. For the molecular modeling software, we thank the CRIHAN, the "Région Haute Normandie" and the European Community (FEDER).

REFERENCES AND NOTES

(1) Martin, G. R.; Humphrey P. P. A, Classification Review Receptors for 5-hydroxytryptamine: Current Perspectives on Classification and Nomenclature. *Neuropharmacol.* **1994**, *33*, 261−273.
(2) Hoyer, D.; Clarke, D. E.; Fozard, J. R.; Harting, P. R.; Martin, G. R.; Mylecharane, E. J.; Saxena, P. R.; Humphrey, P. A. VII International Union of Pharmacology Classification of Receptors for 5-Hydroxytryptamine (Serotonin). *Pharmacol. Rev.* **1994**, *46*, 157−203.
(3) Zifa, E.; Fillion, G. 5-Hydroxytryptamine Receptors. *Pharmacol. Rev.* **1992**, *44*, 401−458.
(4) Saxena, P. R. Serotonin receptors: Subtypes, functional responses and therapeutic relevance. *Pharmac. Ther.* **1995**, *66*, 339−368.
(5) Sanger, G. J.; Nelson, G. R. Selective and functional 5-hydroxytryptamine receptor antagonism by BRL 43694 (Granisetron). *Eur. J. Pharmacol.* **1989**, *159*, 113−124.
(6) Butler, A.; Hill, J. M.; Ireland, S. J.; Jordan, C. C.; Meyers, M. B. Pharmacological Properties of GR 3032F, a novel antagonist at 5-HT3 receptors. *Br. J. Pharmacol.* **1988** *94*, 387−412.
(7) Richardson, B. P.; Engel, G.; Donatsch, P.; Stadler, P. A. Identification of serotonin m-receptor subtypes and their specific blockade by a new class of drugs. *Nature* **1985**, *316*, 126−131.
(8) Aapro, M. S. 5-HT3 receptor antagonists. An overview of their present status and future potential in cancer therapy-induced emesis. *Drugs* **1991**, *42*, 551−568.
(9) Rault, S.; Lancelot, J. C.; Prunier, H.; Robba, M.; Renard, P.; Delagrange, P.; Pfeiffer, B.; Caignard, D. H.; Guardiola-Lemaitre, B.; Hamon, M. Novel selective and Partial Agonists of 5-HT3 Receptors. Part 1. Synthesis and Biological Evaluation of Piperazinopyrrolothienopyrazines. *J. Med. Chem.* **1996**, *39*, 2068−2080.

(10) Prunier, H.; Rault, S.; Lancelot, J. C.; Robba, M.; Renard, P.; Delagrange, P.; Pfeiffer, B.; Caignard, D. H.; Misslin, R. Guardiola-Lemaitre, B. and Hamon, M. Novel selective and Partial Agonists of 5-HT3 Receptors. Part 2. Synthesis and Biological Evaluation of Piperazinopyridopyrrolopyrazines, Piperazinopyrroloquinoxalines, and piperazinopyridopyrroloquinoxalines. *J. Med. Chem.* **1997**, *40*, 1808−1819.
(11) Rault, S.; Robba, M.; Lancelot, J. C.; Prunier, H.; Renard, P.; Pfeiffer, B.; Guardiola, B.; Rettori, M. C. Nouveaux ethers d′oximes tricycliques, leurs procédés de fabrication et les compositions pharmaceutiques qui les contiennent. *Eur. Pat. Appl.* **1994**, no. 9415431.
(12) Higgins, G. A.; Joharchi, N.; Sellers, E. M. Behavioural Effects of the 5-Hydroxytryptamine3 Receptor Agonists 1-phenyl biguanide and *m*-chlorophenylbiguanide in Rats. *J. Pharmacol. Exp. Ther.* **1993**, *264*, 1440−1449.
(13) Barnes, J. M.; Barnes, N. M. Differential binding characteristics of agonists at 5-HT_3 receptor recognition sites in NG 108-15 neuroblastoma-glioma cells labeled by [^{3}H]-(S)-zacopride and [^{3}H] granisetron. *Biochem. Pharmacol.* **1993**, *45*, 2155−2158.
(14) Sharif, N. A.; Wong, E. H. F.; Loury, D. N.; Stefanich, E.; Michel, A. D.; Eglen, R. M.; Whiting, R. L. Characteristics of 5-HT_3 binding sites in NG 108-15, NCB-20 neuroblastoma cells and rat cerebral cortex using [^{3}H]-quipazine and [^{3}H]-GR 65630 binding. *Br. J. Pharmacol.* **1991**, *102*, 919−925.
(15) Glennon, R. A.; Ismael, A. M.; McCarthy, B. G.; Peroutka, S. J. Binding of arylpiperazines to 5-HT_3 serotonin receptors: results of the structure affinity study. *Eur. J. Pharmacol.* **1989**, *168*, 387−392.
(16) Emerit, M. B.; Riad, M.; Fattaccini, C. M.; Hamon, M. Characteristics of [^{14}C]Guanidinium Accumulation in NG 108-15 Cells Exposed to Serotonin 5-HT_3 Receptor Ligands and Substance P. *J. Neurochem.* **1993**, *60*, 2059−2061.
(17) Bureau, R.; Lancelot, J. C.; Prunier, H.; Rault, S. Conformational analysis and 3D QSAR study on novel partial agonists of 5-HT_3 receptors. *Quant. Struct.-Act. Relat.* **1996**, *15*, 373−381.
(18) Daveu, C.; Bureau, R.; Baglin, I.; Prunier, H.; Lancelot, J. C.; Rault, S. Definition of a pharmacophore for partial agonists of serotonin 5-HT3 receptors. *J. Chem. Inf. Comput. Sci.* **1999**, *39*, 362−369.
(19) CATALYST Version 3.0 software; Molecular Simulations Inc.: Burlington, MA, 1993.
(20) Morreale, A.; Galvez-Ruano, E.; Iriepa-Canalda, I.; Boyd, B. D. Arylpiperazines with serotonin-3 antagonists activity: a comparative molecular field analysis. *J. Med. Chem.* **1998**, *41*, 2029−2039.
(21) Cappeli, A.; Anzini, M.; Vomero, S.; Canullo, L.; Mennuni, L.; Makovec, F.; Doucet, E.; Hamon, M.; Menziani, M. C.; De Benedetti, P. G.; Bruni, G.; Romeo, M. R.; Giorgi, G.; Donati, A. Novel potent and selective central 5-HT_3 ligands provided with intrinsic efficacy. 2. Molecular basis of the intrinsic efficay of arylpiperazine derivatives at the central 5-HT_3 receptors. *J. Med. Chem.* **1999**, *42*, 1556−1575.
(22) Cappeli, A.; Anzini, M.; Vomero, S.; Mennuni, L.; Makovec, F.; Doucet, E.; Hamon, M.; Bruni, G.; Romeo, M. R.; Menziani, M. C.; De Benedetti, P. G.; Langer, T. Novel potent and selective central 5-HT_3 ligands provided with intrinsic efficacy. 1. Mapping the central 5-HT_3 receptor binding site by arylpiperazine derivatives. *J. Med. Chem.* **1998**, *41*, 728−741.
(23) Cramer, R. D., III; Patterson, D. E.; Bunce, J. D. Comparative Molecular Field Analysis (CoMFA). 1. Effect of shape on Bindings of Steroids to Carrier Proteins. *J. Am. Chem. Soc.* **1988**, *110*, 5959−5967.
(24) Brooks, B. R.; Bruccoleri, R. E.; Olafson, B. D.; Sates, D. J.; Swaninathan, S.; Karplus, M. CHARMM: A program for macromolecular energy, minimization, and dynamics calculations. *J. Comput. Chem.* **1983**, *4*, 187−217.
(25) DISCOVER 95.0/3.00 software; Molecular Simulations Inc.: Burlington, MA, 1993.
(26) Hibert, M. F.; Hoffmann, R.; Miller, R. C.; Carr, A. A. Conformation-activity relationship study of 5-HT_3 receptor antagonists and a definition of a model for this receptor site. *J. Med. Chem.* **1990**, *33*, 1594−1600.
(27) SYBYL 6.0; Tripos Assocation: St. Louis, MO, 1992.
(28) Bush, B. L.; Nachbar, R. B. *J. Computer-Aided Mol. Design* **1993**, *7*, 587−619.
(29) Cho, S. J.; Tropsha, A. Cross-validated r^2-guided region selection for comparative molecular field analysis: a simple method to achieve consistent result. *J. Med. Chem.* **1995**, *38*, 1060−1066.
(30) Cramer, R. D., III.; Depriest, S. A.; Patterson, D. E.; Hecht, P. The developing practice of Comparative molecular field analysis. In *3D QSAR in Drug Design: Theory, Methods, and Applications*; Kubinyi, H., Ed.; ESCOM: Leiden, 1993; pp 443−485.
(31) LUNDON2; Lundon Software, Inc.: http://www.geocities.com.

CI000058X